J. ICT Res. Appl., Vol. 17, No. 3, 2023, 356-372

A Decoupling Technique for Beamforming Antenna Arrays Using Simple Guard Trace Structures

Zulfi[1,2,*], **Joko Suryana**[1] **& Achmad Munir**[1]

[1]Radio Telecommunication and Microwave Laboratory,
School of Electrical Engineering and Informatics, Institut Teknologi Bandung,
Jalan Ganesha No. 10 Bandung 40132, Indonesia
[2]School of Electrical Engineering, Telkom University,
Jalan Telekomunikasi No. 1 Bandung 40257, Indonesia
*E-mail: zulfi@students.ac.id

Abstract. This paper discusses decoupling techniques for suppressing electromagnetic coupling between elements of beamforming antenna arrays. Guard trace structures, which are commonly used for crosstalk reduction on printed circuit board technology, are proposed to be inserted between the array elements for coupling reduction. Two types of guard trace structures, i.e., straight guard traces and serpentine guard traces, were explored, and the effect of using via holes on both types of guard traces was studied. For this purpose, two-element antenna arrays with guard trace structures inserted between array elements were designed and simulated. The simulation results showed that a straight guard trace with vias (straight GTV) and a serpentine guard trace without vias (serpentine GT) could effectively reduce EM coupling between elements of array antennas. To verify the simulation results, prototypes of antenna arrays with straight GTV and serpentine GT were realized and measured. The measurement results showed coupling reductions of 5 dB and 6.4 dB could be achieved when straight GTV and serpentine GT are inserted between two array elements separated by edge-to-edge distances of 4 mm and 9.05 mm, respectively. Therefore, the proposed decoupling technique is suitable for beamforming antenna arrays with a very close distance between array elements.

Keywords: *beamforming antenna array; EM coupling; microstrip patch antenna; serpentine guard trace; straight guard trace; via hole.*

1 Introduction

The microstrip antenna is the most versatile antenna commonly used in wireless applications. Low weight, ease of fabrication, low implementation cost, and high efficiency are the main advantages of this type of antenna. However, they are inherently narrow-bandwidth and low-gain antennas. To increase the gain, several single microstrip antennas can be arranged to form an array antenna. To achieve beam flexibility of array antennas, electrical steering capability is desired. Technically, antenna arrays with electrical steering capability can be achieved by introducing beamforming techniques [1]. A beamforming antenna

---

Received June 27th, 2023, Revised December 15th, 2023, Accepted for publication December 31st, 2023.
Copyright © 2023 Published by IRCS-ITB, ISSN: 2337-5787, DOI: 10.5614/itbj.ict.res.appl.2023.17.3.5

array leads to maximum and null beam radiation in the desired and undesired directions, respectively. This can be accomplished by driving antenna elements with different phases generated from a beamforming circuit [2]. Beamforming array antennas can be built by utilizing any kind of radiating element. However, printed radiators, such as microstrip patch antennas, are well suited for constructing lightweight and compact beamforming antenna arrays [3]. A further advantage is that they are easy to integrate with a beamforming circuit [4]. Such advantages has motivated microwave designers to pay more attention to microstrip-based beamforming array antennas. However, beamforming antenna arrays using printed antenna technology suffer from EM coupling as a result of the excitation of surface waves, which reduces their gain and maximum scanning angle [5].

Meanwhile, with the increasing need for high-density antenna arrays, massive antenna elements are required. However, since there is limited available space for antennas, adding more antennas will lead to a reduction in antenna spacing. On the other hand, smaller antenna spacing leads to increased coupling intensity between antenna elements, which further deteriorates the performance of array antennas. Therefore, an effective method is needed to suppress EM coupling and enhance the performance of the array antenna. The most straightforward way to minimize the coupling effect in array antennas is increasing the antenna spacing by more than half a wavelength, as recommended in [6]. However, this contrasts with high-density antenna array design requirements. In addition, in array environments, spacing of more than half a wavelength between antenna elements will lead to other issues, such as limited beam steering capability for phased-array antennas and grating lobes.

Various types of decoupling structures have been suggested to disturb the surface current and hence enhance the EM coupling reduction in antenna arrays, including electromagnetic bandgaps [7][8], defective ground structures [9]-[12], and metamaterials [13]-[15]. The aforementioned decoupling structures can effectively reduce EM coupling, but at the expense of being complex in design and fabrication since they are periodic structures that require at least three or more periods to be effective. In addition, in several proposed techniques, the coupling reduction occurs in part of the frequency range, while in other ranges, the coupling effect increases [9]-[11]. Guard trace structures have been frequently used in microwave systems for a range of applications for several decades. Guard traces are widely utilized in PCB circuits for crosstalk reduction between devices on board [16][17]. They have also been used as decoupling structures to minimize EM coupling effects among radiating elements of microstrip array antennas [18]-[24]. However, the guard trace structures used are not simple, which increases the complexity of the antenna structure. This paper proposes simple guard trace structures for suppressing EM coupling between array elements of beamforming antenna arrays.

2 EM Coupling Between Microstrip Patch Antennas

To demonstrate EM coupling between two patch antennas, the configuration shown in Figure 1 was constructed. Two rectangular microstrip antennas, where each antenna patch has width W_a and length L_a, are arranged in a side-by-side configuration with a center-to-center distance of S_c, which corresponds to an edge-to-edge distance of S_e. Each antenna is fed through a microstrip line, which has width W_f and length L_f, respectively, and a transformer line, which has width W_m and length L_m, respectively.

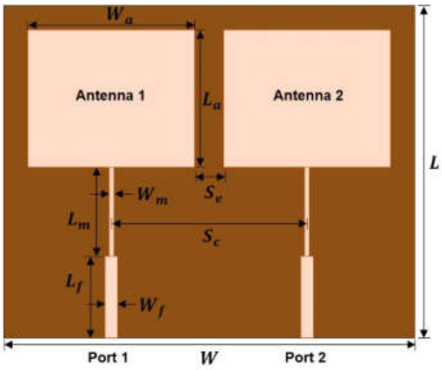

Figure 1 Configuration of a two-element antenna array.

Table 1 Optimized dimensions of antenna configuration.

Parameters	Symbol	Size (mm)
Width of the antenna patch	W_a	34.5
Length of the antenna patch	L_a	28.3
Width of the transformer line	W_m	1.0
Length of the transformer line	L_m	18.3
Width of the feeding line	W_f	2.6
Length of the feeding line	L_f	16.9

The configuration is designed on a 1.6 mm thick FR4 dielectric substrate ($\varepsilon r = 4.4$, $\tan\delta = 0.02$). The antenna dimensions are calculated using the standard microstrip antenna formula at 2.4 GHz. Based on the calculated dimensions, the optimal dimensions of the antenna structure are determined by performing parametric simulations using an electromagnetic simulator, as summarized in Table 1. The simulated scattering parameter response, i.e., the EM coupling represented by transmission coefficient (S_{21}) and reflection coefficient (S_{11}), for different antenna spacings is plotted in Figure 2. As expected, the EM coupling intensity between the antenna elements becomes weaker as the antenna spacing (S_e) increases, as shown in Figure 2(a). Moreover, from Figure 2(b), the reflection coefficient is relatively constant for various antenna spacings.

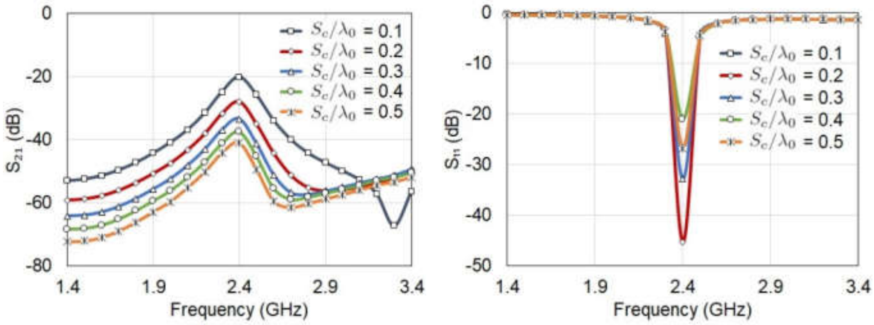

(a) (b)

Figure 2 EM coupling characteristics between microstrip patch antennas (a) transmission coefficient, and (b) reflection coefficient..

3 Reduction of EM Coupling using Guard Trace Structures

In this work, two types of guard trace structures, i.e., straight and serpentine guard traces, are proposed to reduce EM coupling between two antenna elements of an antenna array.

3.1 Straight Guard Trace

The configuration of a two-element antenna array with a straight guard trace is depicted in Figure 3. The structure is composed of two rectangular microstrip antennas and a straight guard trace inserted between the antennas. The straight guard trace is a microstrip transmission line loaded with a number of vias. The microstrip line has a length that is equal to the width of the antenna patches, while the width is W_g. The vias have a diameter of D_v each and are uniformly distributed along the line with a spacing of S_v. To determine the optimum dimensions of the straight guard trace, parametric simulations were carried out for the antenna configuration shown in Figure 3 using an electromagnetic simulator. In the simulations, the distance between antennas was set to 4 mm, which was attributed to $0.032\lambda_0$, where λ_0 is the wavelength of an EM wave propagating in a vacuum. As a result, the optimum configuration was achieved with a straight guard trace width of 3 mm, a via spacing of 8.6 mm (4 vias), and a via diameter of 1 mm.

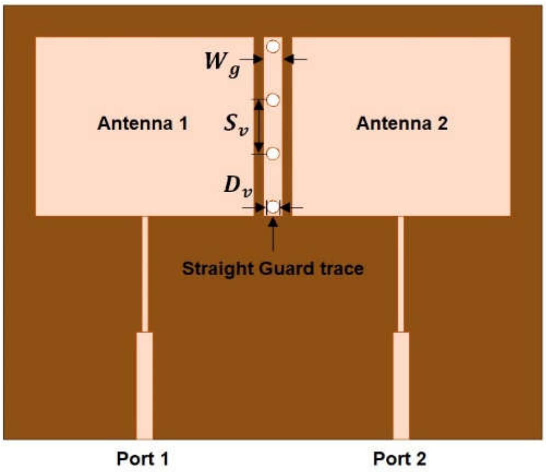

Figure 3 Configuration of a two-element antenna array with a straight guard trace.

To analyze the impact of using a straight guard trace, a two-element array with and without a straight guard trace in between were simulated using an EM simulator. The simulated scattering parameter is depicted in Figure 4. It can be seen that the insertion of a straight guard trace without vias (straight GT) between antenna patches cannot suppress EM coupling. In contrast, placing a straight guard trace with vias (straight GTV) between antenna patches reduces the coupling intensity over the entire frequency range, as shown in Figure 4(a). At 2.4 GHz, the transmission coefficient of the two-element array with a straight GTV is −17.3 dB, while without GT it is −12.7 dB, indicating a 4.6 dB coupling reduction. Moreover, it was found that introducing a straight guard trace with via among antenna patches improves impedance matching at the expense of a very small frequency shift, as depicted in Figure 4(b).

The resonant frequencies of a two-element array with and without GTV were 2.44 GHz and 2.42 GHz, respectively, corresponding to a 20 MHz frequency shift. A straight GTV made of conducting material placed between the two antennas is like a parasitic antenna that exists between the two antennas. The interaction of straight GTV with both antennas produces mutual coupling. Due to the different dimensions, the mutual coupling that occurs between the straight GTV and the two antennas has a different resonance frequency from the coupling resulting from the interaction between the antennas. The total coupling on one antenna comes from the coupling resulting from interaction with the straight GTV and the coupling resulting from interaction with the antenna. Therefore, an antenna array with a straight GTV has a different resonance frequency than an antenna array without a straight GTV.

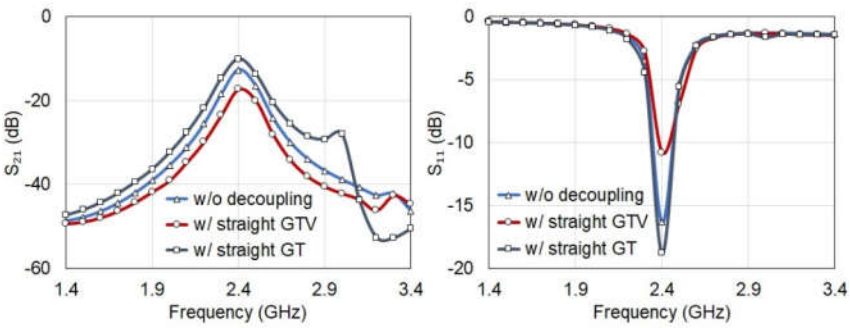

(a) (b)

Figure 4 Simulated results of the scattering parameters (a) transmission coefficient, and (b) reflection coefficient.

To explain the EM coupling reduction, the current distribution for the antennas with and without a straight guard trace is plotted in Figure 5. It can be seen that by inserting a straight guard trace between antenna patches, the coupled EM waves from Antenna 1 are bound to the straight guard trace structure instead of being coupled to Antenna 2. Hence, a lower concentration of surface currents is found in Antenna 2, as shown in Figure 5(a), which indicates weak coupling among the antennas. Figure 5(b) depicts the current distribution on antennas without straight guard trace. A higher current concentration appears on Antenna 2, indicating strong coupling between the antennas.

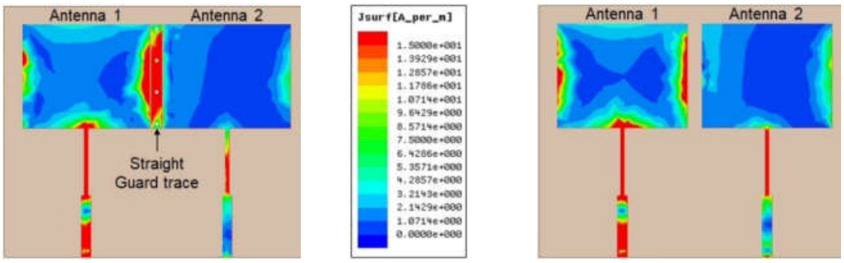

(a) (b)

Figure 5 Current distributions on antenna (a) with straight guard trace, and (b) without straight guard trace.

To validate the impact of the proposed decoupling approaches, further investigations were done. Some results related to antenna parameters (gain and efficiency, and MIMO parameters), i.e., the envelope correlation coefficient (ECC) and the diversity gain (DG), are plotted in Figure 6. A small difference in gain and efficiency between the antenna arrays with and without decoupling structures was observed. For all three configurations, their gain and efficiency were about -1 dBi and 50%, respectively, as shown in Figures 6(a) and 6(b). Low gain and poor efficiency are due to the large dielectric loss of the FR-4 dielectric material used in the design. The antenna arrays with straight GTV had the lowest EEC (Figure 6(c)) and the highest diversity gain (Figure 6(d)). The results indicate that the decoupling technique using straight GTV could improve MIMO antenna performance.

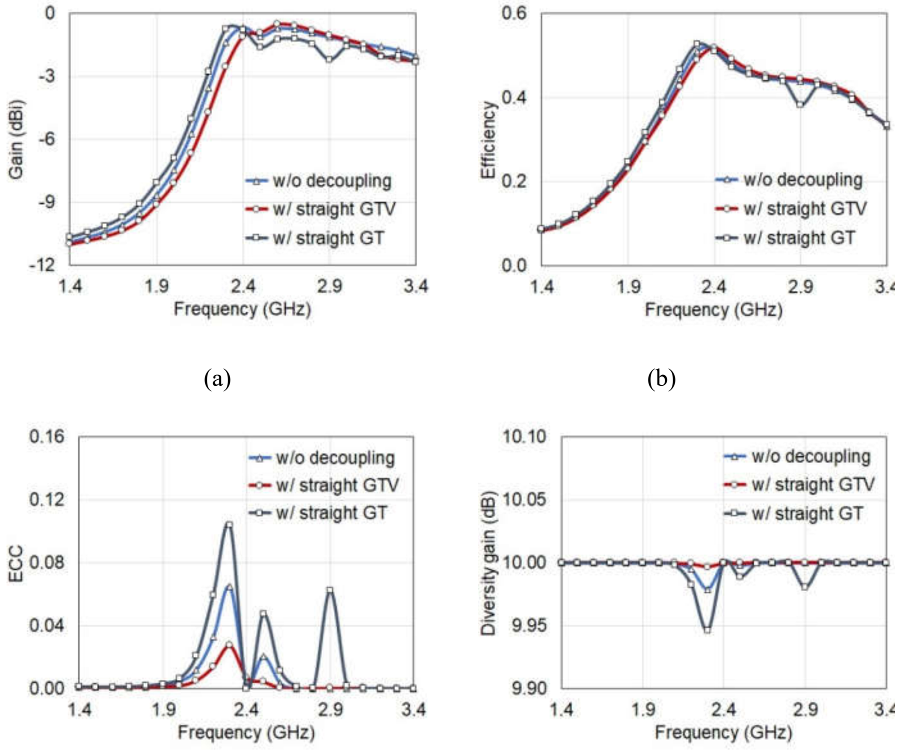

(a) (b)

(c) (d)

Figure 6 Simulation results for (a) gain, (b) efficiency, (c) EEC, and (d) diversity gain.

3.2 Serpentine Guard Trace

Figure 7 illustrates the antenna configuration with a serpentine guard trace in between. The serpentine guard trace is a meandering microstrip line that has a width of W_s, a gap separation of L_h, a height of L_v, and a length equal to the width of the antenna patch (W_a). To determine the optimum dimensions for the serpentine guard trace, parametric simulations were carried out using an electromagnetic simulator. In the simulations, the separation distance between antenna patches was set to 9.05 mm. As a result, the optimum configuration was achieved with a serpentine guard trace width of 1.7 mm, a gap separation of 1.575 mm, a height of 3.9 mm, and a length of 28.2 mm.

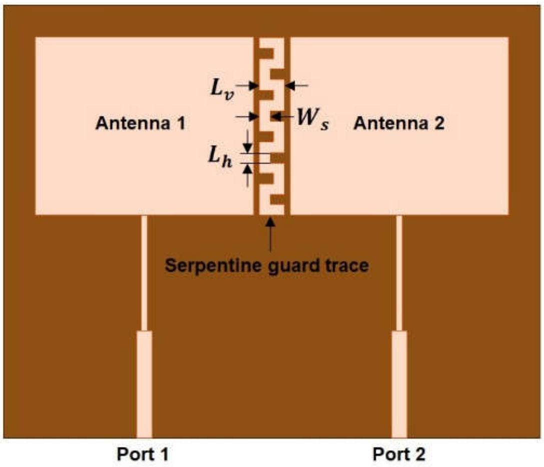

Figure 7 Configuration of antenna with serpentine guard trace.

Figure 8 depicts the simulation results for the scattering parameters, i.e., the transmission and reflection coefficients. The simulated transmission coefficient is shown in Figure 8(a). It was found that inserting a serpentine guard trace with vias (serpentine GTV) between patches did not significantly decrease the coupling intensity. In contrast, introducing a serpentine guard trace without vias (serpentine GT) between antenna patches suppressed EM coupling in the frequency range from center to high frequencies. At a frequency of 2.4 GHz, the transmission coefficients of the two-element array with and without serpentine GT were −25.0 dB and −17.4 dB, respectively, demonstrating a 7.6 dB coupling reduction. The simulated reflection coefficients are plotted in Figure 8(b). It can be seen that introducing a serpentine GTV among the antenna patches slightly reduced the impedance matching and shifted the resonant frequency. Resonant frequencies with and without a guard trace were 2.40 GHz (S_{11} = −32 dB) and

2.42 GHz ($S_{11} = -28$ dB), respectively, showing a 20 MHz frequency shift and a 4 dB decrease in impedance matching.

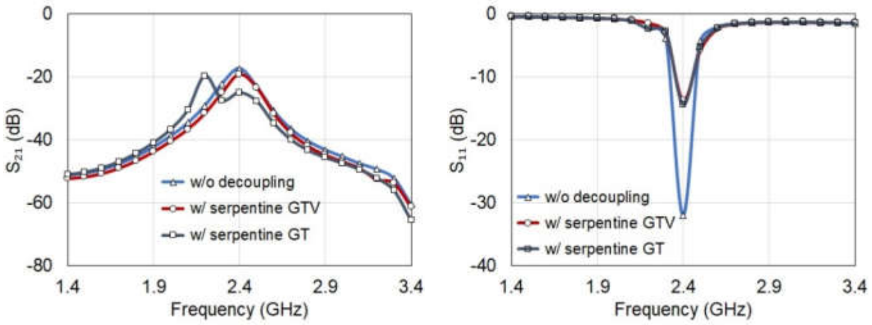

(a) (b)

Figure 8 Simulation results of scattering parameters (a) transmission coefficient, and (b) reflection coefficient.

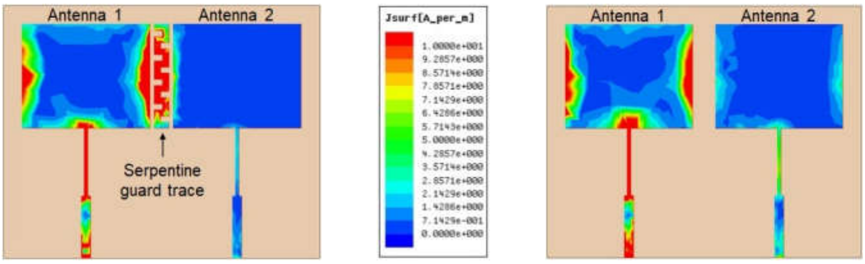

(a) (b)

Figure 9 Current distributions on antenna (a) with serpentine guard trace and (b) without serpentine guard trace.

The current distribution for the antennas with and without a serpentine guard trace is illustrated in Figure 9. It can be seen that by introducing a serpentine guard trace between antenna patches, the coupled EM waves from Antenna 1 are bound to the guard trace structure instead of being coupled to Antenna 2. Hence, a lower concentration of surface currents was found in Antenna 2, as shown in Figure 9(a), which indicates weak coupling among the antennas. Figure 9(b) depicts the current distribution in antennas without a serpentine guard trace. A higher current concentration appeared on Antenna 2, indicating strong coupling between the antennas.

Figure 10 shows the simulated results for gain, efficiency, envelope correlation coefficient (ECC), and diversity gain (DG) of antenna arrays with and without serpentine guard trace. For the case of the antenna array with serpentine GT, a degradation in gain, efficiency, EEC, and diversity gain at 2.2 GHz was observed. However, within a 10-dB reflection coefficient bandwidth, the performance of the antenna array with serpentine GT was outperformed. The antenna array with a serpentine GT had the lowest EEC (Figure 10(c)) and the highest diversity gain (Figure 10(d)). The results indicate that the decoupling technique using serpentine GT could improve MIMO antenna performance.

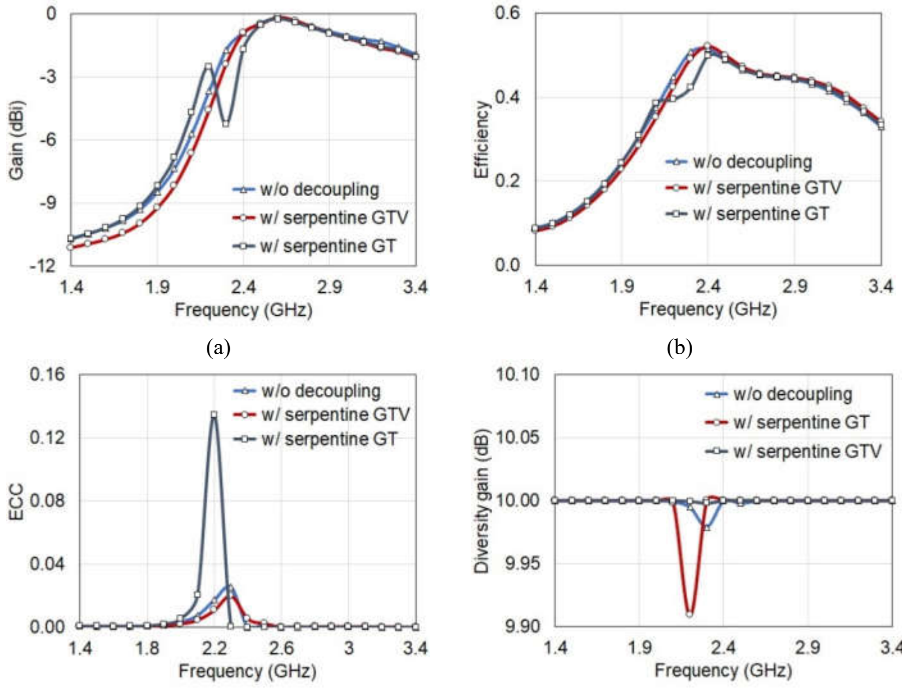

(a) (b)

(c) (d)

Figure 10 Simulation results for (a) gain, (b) efficiency, (c) EEC, and (d) diversity gain.

4 Experimental Verification

Based on the simulation results discussed in Section 3, the antenna array with a straight GTV and a serpentine GT could provide a greater EM coupling reduction compared to a straight GT and a serpentine GTV. Therefore, prototypes of antenna arrays with a straight GTV and a serpentine GT were realized and measured for experimental verification. Figures 9(a) and 11(a) show photographs of the antenna prototypes with a straight guard trace with vias and a serpentine guard trace, respectively, realized on a 1.6 mm thick FR4 printed circuit board. Furthermore, the fabricated prototypes were measured. Figures 11(b) and 13(b) depict the measurement setup of the antenna configuration with a straight and a serpentine guard trace, respectively. For measurement purposes, the antenna ports were attached with 50-Ω SMA connectors. The scattering parameters, i.e., the transmission and reflection coefficients, were tested within a 1.4 to 3.4 GHz frequency range using a vector network analyzer.

4.1 Straight Guard Trace with Via

Figure 12 illustrates the measurement and simulation results for the scattering parameters for an antenna with a straight guard trace. The measurement results agreed with the simulation ones. At 2.4 GHz, the measured transmission coefficient was –18.7 dB, while the simulated result was –17.3 dB, as shown in Figure 12(a). Hence, a 1.4 dB difference in transmission coefficient was observed. The reflection coefficient response is plotted in Figure 12(b). The measured resonant frequency was 2.49 GHz, while the simulated result was 2.44 GHz, corresponding to a frequency difference of 50 MHz. The discrepancies observed between the measurement and the simulation results were due to the large dielectric loss of the FR4 PCB, connector loss, fabrication tolerances, and measurement errors.

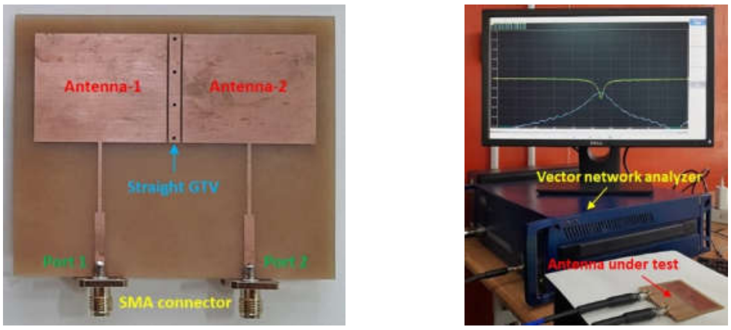

(a) (b)

Figure 11 Photograph of experimental characterization of an antenna with a straight guard trace: (a) fabricated antenna, and (b) measurement setup.

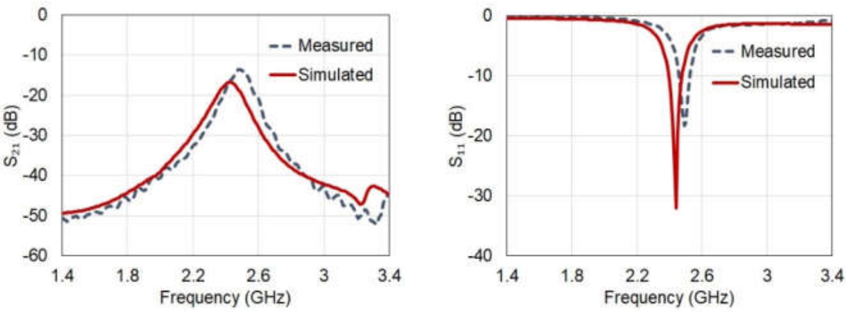

(a) (b)

Figure 12 Measured scattering parameters of antenna with straight guard trace: (a) transmission coefficient, and (b) reflection coefficient.

4.2 Serpentine Guard Trace

Figure 14 plots the measurement and simulation results of the scattering parameters for an antenna with a serpentine guard trace. The measurement results agreed with the simulation ones. As depicted in Figure 14(a), the measured and simulated transmission coefficients were –25.9 dB and –25.0 dB, respectively, at 2.4 GHz, corresponding to a 0.9 dB transmission coefficient difference. The reflection coefficient response is shown in Figure 14(b). The measured resonant frequency was 2.48 GHz, while the simulated result was 2.42 GHz, indicating a small resonant frequency shift of 60 MHz.

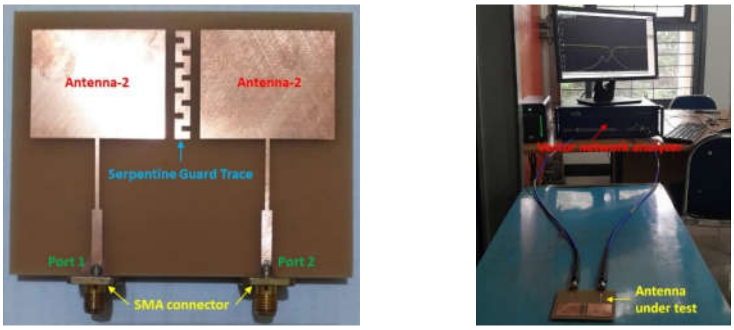

(a) (b)

Figure 13 Photograph of experimental characterization of antenna with serpentine guard trace: (a) fabricated antenna, and (b) measurement setup.

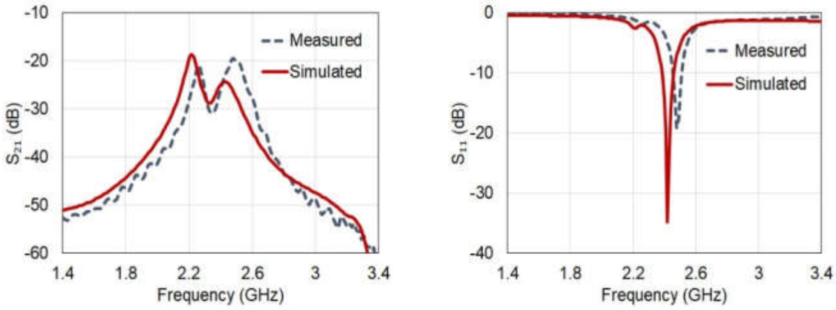

(a) (b)

Figure 14 Measured scattering parameters of antenna with serpentine guard trace: (a) transmission coefficient, and (b) reflection coefficient.

In order to demonstrate the distinctive characteristics of the proposed design, some key performance parameters of an array antenna, i.e., the array dimensions, antenna spacing (edge-to-edge spacing), fractional 10-dB reflection coefficient bandwidth, mutual coupling reduction, and complexity of the antenna configuration, were compared with the data of previously published related works, as tabulated in Table 2.

Table 2 Comparison of proposed antenna designs with related works.

Ref.	Decoupling technique	Array dimensions (λ_0^2)	Antenna spacing (λ_0)	Fractional bandwidth (%)	Coupling reduction (dB)	Complexity
[15]	Frequency selective surface (FSS)	1.84×1.84	0.13	2.6	3.6	Moderate
[7]	Combined EBG and DGS	0.88×0.44	0.13	4.7	20	High
[21]	Open stub meandered BSF	0.96×0.48	0.19	1.2	37	High
[14]	Waveguided Metamaterials	1.06×0.89	0.12	1.4	≥ 6	Moderate
[8]	Electromagnetic bandgap (EBG)	1.93×0.97	0.75	1.7	7.8	Moderate
[9]	Defected Ground Structure (DGS)	1.09×0.78	0.15	5.1	2–5	Moderate
[22]	Slotted Meander-Line Resonators	0.86×0.72	0.11	5.2	6–16	Moderate
This work	Straight guard traces with via	0.66×0.55	0.03	2.9	3.5–5.4	Low
	Serpentine guard traces	0.71×0.55	0.07	2.5	5.8–8.1	Low

The proposed antenna has a higher coupling reduction than the antennas in [15] and [9], and a wider fractional 10-dB reflection coefficient bandwidth than those in [8], [14], and [21] and is comparable to that of the antenna in [15]. In contrast, the proposed design has a lower coupling reduction than the designs reported in [7-9], [14], and [21] and a narrower fractional 10-dB reflection coefficient bandwidth than the designs in [7], [9], and [22]. However, they have large array dimensions and high complexity. The proposed antenna has the smallest array dimension and the lowest complexity and hence is suitable for high-density antenna arrays.

5 Conclusion

A decoupling technique for suppressing EM coupling between elements of beamforming antenna arrays was presented in this paper. To reduce the EM coupling, guard trace structures commonly used to reduce crosstalk on PCB technology are proposed to be inserted between the array elements. To demonstrate the effectiveness of guard trace utilization, two-element antenna arrays with straight GTV and serpentine GT were designed, realized, and measured. The measurement results showed that coupling reductions of 5 dB and 6.4 dB could be achieved at 2.4 GHz when straight and serpentine guard traces were placed between two array elements separated by an edge-to-edge distance of 4 mm and 9.05 mm, respectively. Inserting a straight GTV and a serpentine GT between antenna array elements had little effect on the impedance matching characteristics. Since the strongest coupling reduction occurs at very close element spacings, the proposed decoupling technique is suitable for massive-element beamforming antenna arrays.

Acknowledgement

This work was partially supported by the Indonesian Endowment Fund for Education (Lembaga Pengelola Dana Pendidikan-Beasiswa Unggulan Dosen Indonesia Dalam Negeri, LPDP-BUDI DN) from the Ministry of Finance, Republic of Indonesia, under contract KET-6645/LPDP.4/2022.

Nomenclature

D_v = Diameter of via
L_a = Length of microstrip patch antenna
L_f = Length of feeding line
L_h = Gap separation of serpentine guard trace
L_m = Length of transformer line
L_v = Height of serpentine guard trace
S_c = Center-to-center distance
S_e = Edge-to-edge distance

S_v = Distance between two vias
W_a = Width of microstrip patch antenna
W_f = Width of feeding line
W_g = Width of straight guard trace
W_m = Width of transformer line
W_s = Width of serpentine guard trace

References

[1] Balanis, C.A., *Antenna Theory Analysis and Design*, 4th ed., John Wiley and Son's Inc., 2015.

[2] Bellofiore, S., Foutz, J., Balanis, C.A. & Spanias, A.S., *Smart-Antenna System for Mobile Communication Networks. Part 2, Beamforming and Network Throughput*, IEEE Antennas and Propagation Magazine, **44**(5), pp. 106-114, 2002.

[3] Taha, Z., Jassim, H., Ahmed, A. & Farhan, I., *Design and Implementation of Triple Band Half Mode Substrate Integrated Waveguide (HMSIW) Antenna with Compact Size,* J. ICT Res. Appl., **15**(2), pp. 120-138, 2021.

[4] Dahri, M.H., Jamaluddin, M.H., Khalily, M, Abbasi, M.I., Selvaraju, R. & Kamarudin, M.R., *Polarization Diversity and Adaptive Beamsteering for 5G Reflectarrays: A Review*, IEEE Access, **6**, pp. 19451-19464, 2018.

[5] Chen, X., Abdullah, M., Li, Q., Li, J., Zhang, A. & Svensson, T., *Characterizations of Mutual Coupling Effects on Switch-Based Phased Array Antennas for 5G Millimeter-Wave Mobile Communications,* IEEE Access, **7**, pp. 31376-31384, 2019.

[6] Mohammadian, A.H., Martin, N.M. & Griffin, D.W., *A Theoretical and Experimental Study of Mutual Coupling in Microstrip Antenna Arrays*, IEEE Transactions on Antennas and Propagation, **37**(10), pp. 1217-1223, 1989.

[7] Liu, Y., Yang, X., Jia, Y. & Guo, Y.J., *A Low Correlation and Mutual Coupling MIMO Antenna*, IEEE Access, **7**, pp. 127384-127392, 2019.

[8] Yang, F. & Rahmat-Samii, Y., *Microstrip Antennas Integrated with Electromagnetic Band-Gap (EBG) Structures: A Low Mutual Coupling Design for Array Applications,* IEEE Transactions on Antennas and Propagation, **51**(10), pp. 2936-2946, 2003.

[9] Zulkifli, F.Y., Rahardjo, E.T. & Hartanto, D., *Mutual Coupling Reduction using Dumbbell Defected Ground Structure for Multiband Microstrip Antenna Array*, Progress in Electromagnetics Research Letters, **13**, pp. 29-40, 2010.

[10] Wei, K., Li, J.Y., Wang, L., Xing, Z.J. & Xu, R., *Mutual Coupling Reduction of Microstrip Antenna Array by Periodic Defected Ground*

Structures, 2016 IEEE 5th Asia-Pacific Conference on Antennas and Propagation (APCAP), pp. 389-390, 2016.

[11] Niu, Z., Zhang, H., Chen, Q. & Zhong, T., *Isolation Enhancement for 1×3 Closely Spaced E-Plane Patch Antenna Array using Defect Ground Structure and Metal-Vias,* IEEE Access, **7**, pp. 119375-119383, 2019.

[12] Gao, D., Cao, Z.X., Fu, S.D., Quan, X. & Chen, P., *A Novel Slot-Array Defected Ground Structure for Decoupling Microstrip Antenna Array*, IEEE Transactions on Antennas and Propagation, **68**(10), pp. 7027-7038, 2020.

[13] Zhang, Q.L., Jin, Y.T., Feng, J.Q., Lv, X. & Si, M., *Mutual Coupling Reduction of Microstrip Antenna Array using Metamaterial Absorber*, 2015 IEEE MTT-S International Microwave Workshop Series on Advanced Materials and Processes for RF and THz Applications (IMWS-AMP), pp. 1-3, 2015.

[14] Yang, X.M., Liu, X.G., Zhou, X.Y. & Cui, T.J., *Reduction of Mutual Coupling between Closely Packed Patch Antennas using Waveguided Metamaterials*, IEEE Antennas and Wireless Propagation Letters, **11**, pp. 389-391, 2012.

[15] Hassan, T., Khan, M.U., Attia, H. & Sharawi, M.S., *An FSS based Correlation Reduction Technique for MIMO Antennas*, IEEE Transactions on Antennas and Propagation, **66**(9), pp. 4900-4905, 2018.

[16] Zhi, L., Qiang, W. & Changsheng, S., *Application of Guard Traces with Vias in the RF PCB Layout*, 2002 3rd International Symposium on Electromagnetic Compatibility, pp. 771-774, 2002.

[17] Suntives, A., Khajooeizadeh, A. & Abhari, R., *Using via Fences for Crosstalk Reduction in PCB Circuits,* 2006 IEEE International Symposium on Electromagnetic Compatibility (EMC 2006), pp. 34-37, 2006.

[18] Park, C.H. & Son, H.W., *Mutual Coupling Reduction between Closely Spaced Microstrip Antennas by Means of H-Shaped Conducting Wall,* Electronics Letters, **52**(13), pp. 1093-1094, 2016.

[19] Zulfi, Suryana, J., Nur, L.O. & Munir, A., *Investigation of Guard Trace Utilization for EM Coupling Reduction between Closely-Spaced Microstrip Patch Antennas*, 2023 International Symposium on Electromagnetic Compatibility – EMC Europe, pp. 1-6, 2023.

[20] Zulfi, Adriansyah, N.M., Suryana, J. & Munir, A., *Envelope Correlation Evaluation of MIMO Antenna with Guard Trace Structures*, 2023 28th Asia Pacific Conference on Communications (APCC), pp. 1-5, 2023.

[21] Govindarajulu, S.R., Jenkel, A., Hokayem, R. & Alwan, E.A., *Mutual Coupling Suppression in Antenna Arrays using Meandered Open Stub Filtering Technique*, IEEE Open Journal of Antennas and Propagation, **1**, pp. 379-386, 2020.

[22] Alsath, M.G.N., Kanagasabai, M. & Balasubramanian, B., *Implementation of Slotted Meander-Line Resonators for Isolation Enhancement in Microstrip Patch Antenna Arrays*, IEEE Antennas and Wireless Propagation Letters, **12**, pp. 15-18, 2013.

[23] Zulfi & Munir, A., *Reduction of Electromagnetic Coupling between Patch Antennas using Meander Line Structure*, 2023 IEEE 7th Global Electromagnetic Compatibility Conference (GEMCCON), pp. 72-72, 2023.

[24] Zulfi, Arseno, D. & Munir, A., *Suppression of EM Coupling between Microstrip Patch Antennas using a Simple Meander Line Structure*, 2023 IEEE International Symposium on Antennas and Propagation and USNC-URSI Radio Science Meeting (USNC-URSI), pp. 1455-1456, 2023.